N-body Simulations in Galactic Potentials

David Andersson

February 4, 2019

Abstract

What effect does a collision between two clusters have on their dissolving time?

In order to answer this question, a new type of N-body simulation using a double integration of a cluster was built. Instead of introducing a perturbation representing the gravitational force of the Milky Way into a local simulation of the cluster, the cluster orbit was integrated in the potential of the Milky Way, and in each of these integration steps the local motion of the stars inside the cluster were integrated, using an N-body calculation. The goal of this new type of integrator was to create a more versatile and intuitive simulation, where no perturbation calculation was needed before initiating a cluster. The simulation as a whole was tested using different resolutions and relative tolerances, and both the N-body calculation and potential integration were tested separately as well as in conjunction.

As a test subject, the Hyades open cluster was investigated in this project. The number of stars within the tidal radius of the cluster as a function of time was calculated, and the effect of cluster collisions on the decay rate was investigated. The results are also highly indicative of that the star HD31236 is not an actual member of the Hyades, though this needs further testing, taking the formal errors of the initial conditions into account.

Populärvetenskaplig beskrivning

För att förstå vårt ursprung och vår plats i universum, måste vi först lära oss om vår historia. Detta är en utmaning i många fält inom vetenskapen, och det finns ett antal olika tillvägagångssätt; geologer analyserar sedimentlager för att få förstå vår planets utveckling, biologer tittar på små skillnader i flora och fauna för att förstå utvecklingen av arter, och paleontologer undersöker fossil från länge utdöda arter för att kunna göra detsamma. Den gemensamma nämnaren i dessa tre fallen är att tidsskalorna för dessa processer långt överskrider tidsskalan för mänsklig historia, så istället för att observera t.ex en art under hela vår jords historia, så tittar vi på liknande arter från olika tidsåldrar, och gör antagandet att den ena utvecklades från den andra. Det påminner mycket om att lösa ett vetenskapligt pussel, där varje pusselbit respresenterar en art från en viss tidsålder.

På samma sätt jobbar astronomer och astrofysiker för att förstå vår galax Vintergatans utveckling, men eftersom tidsskalorna är ännu större än de för vår jord så måste ännu mer information till innan vi kan skapa teorier om hur den utvecklats. Detta är problematiskt, eftersom observationsutrustning som t.ex teleskop är dyra, för att inte tala om en teknisk utmaning. Men med den senaste utvecklingen inom beräkningskraft har astronomer och astrofysiker fått ett nytt verktyg som hjälper till att hålla kostnader nere och öka vår förståelse för vår omgivning; simulationer!

Eftersom de fysiska lagar som styr vår galax och hur saker rör sig i rymden har varit kända sen Newtons dagar (med några senare modifikationer and tillägg, främst från Einstein), så har vi kunnat räkna ut planeters och stjärnors banor i århundraden. Den stora skillnaden har kommit de senaste årtiondena, i form av den exponentiellt ökande beräkningskraften hos datorer. Detta gör att vi kan utföra mer och mer avancerade uträkningar, och en av dessa är så kallade N-body-simuleringar (av engelskans N *bodies*, N kroppar). Dessa simuleringar beräknar hur inte bara två objekt, utan många hundratals objekt interagerar med varandra gravitationsmässigt, och ger oss möjligheten att utforska olika scenarion bara genom att bestämma var dessa objekt är just nu, och hur de rör sig.

Stjärnor i vår galax samlar ofta ihop sig eller skapas i grupper av upp till tusentals, som kallas stjärnhopar. Dessa stjärnhopar är bundna till varandra genom gravitation, och kretsar kring varandra, såväl som runt Vintergatans mitt. För att förstå hur dessa stjärnhopar blivit till, hur de rör sig och hur de en dag kommer lösas upp, behöver vi förstå både hur stjärnorna inuti hopen rör sig, men också hur de rör sig i den stora Vintergatan. Det är här N-body-simuleringar kommer in; genom att beräkna hur stjärnorna dras till varandra genom gravitationen, kan vi undersöka hur stjärnhopar rör sig och faller isär, och genom att simulera bakåt i tiden kan vi förstå hur de en gång skapades.

Allt eftersom beräkningskraften ökar kan vi simulera fler och fler interaktioner mellan individuella stjärnor i dessa hopar. Dessa N-body-simuleringar ger en mer och mer sanningsenlig respresentation av vad som egentligen händer i en stjärnhop; en ”bättre upplöst bild”, eftersom dessa stjärnor kommer att interagera med varandra. Detta ger oss en stor och viktig pusselbit i pusslet som vi kallar Vintergatans utveckling.

Contents

List of Figures

List of Tables

Chapter 1

Introduction

During the last 20 years a lot has happened within the field of astrometry. When the results of the HIPPARCOS satellite became available in 1997, the absolute parallax of over 117 000 objects had been measured with milli-arcsecond accuracy (Perryman et al. 1997a), compared to the 8000 objects for which ground-based parallaxes were available before this. This enabled researchers to expand our knowledge of stellar structure and evolution, as well as increase our understanding of dynamical astronomy and stellar kinematics.

The next major step in this rapid advance in astrometry will be the full data release of the GAIA mission, estimated to be released in 2022 or 2023. This release will contain highly accurate astrometric parameters (positions, parallaxes and proper motions) for over a billion objects in the Milky Way down to a GAIA-magnitude of $G = 20.7$ mag (Prusti et al. 2016), as well as the radial velocities of stars with a GAIA-magnitude of $G \approx 17$ mag or lower (Brown et al. 2016). The GAIA mission has already contributed with astrometric data through intermediate data releases called GAIA Data Release 1 & 2 (DR1 & 2). In 2016, data gathered by the mission so far was released (GDR 1), with the downside of not being able to guarantee the accuracy of the full data release (more information can be found in Brown et al. (2016)). DR1 contains positions, parallaxes and mean proper motions for about 2 million objects, as well as positions for an additional 1.1 billion sources. A second intermediate data release was released in April 2018, with improved accuracy, and contains positions, proper motions and parallaxes of 1.3 billion objects with a Gaia magnitude between $G \approx 3$ and $G = 21$ (ESA 2018).

The GAIA mission has and will contribute a lot in the field of observational astronomy. According to Prusti et al. (2016) the primary focus of the mission is to increase our knowledge of our own galaxy, the Milky Way, but the GAIA data is being used in a wide array of subjects in the field, even before its final release. By taking astrometric measurements of objects in our galaxy and analysing the kinematics and distribution of both visible matter and dark matter, we will be able to draw conclusions about the structure and evolution of the Milky Way. This is possible even though only about 1% of the stars in our galaxy

have been measured, since a great number of stars of different types and classifications are included. Let us also remind ourselves, that even as little as 1% of 100 billion stars is still a billion stars(!). Because of this great sample size of objects, statistical analysis can be used effectively to draw conclusions, even though far from all the stars have been astrometrically measured.

The structure and evolution of the Milky Way is still somewhat of a mystery to science. The theories we have today of its structure are largely based on observations of other galaxies, and these are accompanied by a lot of uncertainty. Because of the grand time scales in astronomy, there is no possibility to observe one galaxy's evolution, so a number of galaxies of the same class are observed at what is presumed to be different steps in their evolution. This method has a downside in that it relies heavily on that our classification system works, i.e. that the galaxies we assume to be similar in origin but at different stages in their evolution really are. This, combined with the difficulties of observing our own Milky Way from an outside perspective, constitutes the major problems when it comes to analysing the structure and evolution of our galaxy.

A powerful and important tool to solve this problem is to perform simulations of galactic evolution, based on astrometric data and the physical laws that govern galaxies. The theories of gravity and the interaction between astronomic bodies have been established since many hundreds of years, but in the last decades computing power has increased exponentially. This has enabled large-scale simulations of galaxies, with thousands or millions of independent bodies. By experimenting with the initial conditions and changing the parameters of galaxies, a lot has been learned about the physical processes behind galaxy formation and evolution. The theories that are put forward can be compared to observations, to hopefully explain the features we observe. This numerical approach to learning more about the history of galaxies has become essential in astronomy over the last decades, and is one of the reasons that the GAIA mission is so important.

The purpose of this project is to simulate astronomical bodies in gravitational potentials, and the project can be divided into subparts. The first part consists of integrating the orbit of a circular nearby cluster in the potential of the Milky Way. Secondly, a number of stellar orbits are initiated in the cluster potential as massless tracer particles. In order to perform both of these steps, astrometric data from GAIA Data Release 1 is used for the initial conditions of the orbits. The third step is to introduce an N-body simulation for the stars in the cluster, so that they now have a mass and affect each other gravitationally. The fourth and final step is to integrate the movement of the stellar orbits in the cluster, while simultaneously integrating the orbit of the cluster in the galactic potential.

The result of this will be an orbital simulation of a cluster in a galactic potential, with many interesting applications. The galactic potential in the simulation will be almost axisymmetric, with the exception of the cluster potential addition in the outskirts of the galactic potential. Since gravitational potentials have a very simple form, it is also relatively simple to introduce other density variations in the galactic potential, such as spiral arms or other star clusters. These can then be used to simulate how clusters are affected when passing

through each other or one of these arms; do they tear apart, becoming gravitationally unbound, or are they largely unaffected by this shift in gravitational potential? To what degree is the rate of star loss affected by the large density variations throughout its orbit around the galactic centre?

The inclusion of an N-body simulation inside the cluster allows for interaction between individual stars, which may cause stars to become gravitationally unbound due to the gravitational potential of other nearby stars. This of course increases the accuracy of the simulation, and allows for some interesting aspects in and of itself. As an example, the previously mentioned application of to what degree the rate of star loss is affected by large density variations will become more accurate if the stars affect each other gravitationally. Since the gravitational potential of the galaxy is approximated as constant at the radius of the cluster, all orbits that are stable will continue to be so if the stars are initiated as tracer particles. It is only when the stars affect each other gravitationally that star leakage may be observed in between major density fluctuations. In other words, the inclusion of an N-body simulation increases the accuracy of the simulation, and is a must for some applications.

Chapter 2

Theory

2.1 The Hyades

The cluster in focus in this project is the Hyades, an open cluster with a mass of about $400M_{\odot}$ at a distance of roughly 40-50 parsec from the solar system, (Perryman et al. 1997b). This makes it one of the nearest open clusters to us, and due to this proximity, the Hyades has been identified and studied since at least ancient Greece (where the name stems from), and has been included in star charts since the 17th century. It was catalogued by Melotte in 1915, who gave it the identification Mel25, an identification that persists to this day. It is also believed to share its origin with Praesepe, the Beehive cluster (M44), as indicated by its age and stellar content, as well as being connected to the Hyades stream (Frommert & Kronberg 2001). In recent times it has been one of many subjects of astrometric data collection using the Gaia Satellite.

The cluster contains up to 300 members, where the central group of the cluster has a radii of roughly 1.5 pc, with members up to 12 pc from the cluster centre. It is believed to be between 600 to 800 Myr old (Perryman et al. 1997b), though more recent studies points towards it being in the very end of this span (790 Myr according to the Hertzsprung-Russell diagram of the cluster (Frommert & Kronberg 2001)). According to "Gravitational N-body Problem, Proceedings of Iau Colloquium No.10", edited by Lecar (1972), only 10% of open cluster exceed an age of 400 Myr, and only 1% exceed an age of 1 Gyr. This means that the Hyades is likely at the end of its lifetime, and if so, should show signs of dissolving. This is the main focus of this project; to investigate the dissolving of the Hyades and the effect of collisions on the dissolving process.

In order to do this, the members of the cluster must first be established. The membership status of stars in the neighbourhood of the Hyades have been studied in great detail, and a very nice summary of these can be found in Table 2 in Perryman et al. (1997b), which was the last major study of the subject. However, this paper was written in 1997, well before

the first Gaia Data Release, and so more accurate astrometric data has become available since. This is the other part of the project; to investigate whether or not any of the stars included in this project are likely not to be real members of the Hyades, given the new astrometric data. (This was not a part of the project from the start, but was investigated further when results indicated stars with very high local velocities.)

2.2 Solving the Equation of Motion ODE

The equation to solve in order to produce a dynamical simulation is the equation of motion. When dealing with an object moving in a gravitational potential in three dimensions, the equation of motion is a system of three second-order Ordinary Differential Equations (ODE's for short) in the form of

$$\bar{a} = \begin{cases} \frac{d^2x}{dt^2} = -\frac{\partial \psi}{\partial x} \\ \frac{d^2y}{dt^2} = -\frac{\partial \psi}{\partial y} \\ \frac{d^2z}{dt^2} = -\frac{\partial \psi}{\partial z} \end{cases} \tag{2.1}$$

where $\psi(x, y, z)$ is the gravitational potential. We can simplify this into a system of six first-order ODE's;

$$\bar{v} = \begin{cases} \frac{dx}{dt} = v_x \\ \frac{dy}{dt} = v_y \\ \frac{dz}{dt} = v_z \end{cases} \tag{2.2}$$

$$\bar{a} = \begin{cases} \frac{dv_x}{dt} = -\frac{\partial \psi}{\partial x} = a_x \\ \frac{dv_y}{dt} = -\frac{\partial \psi}{\partial y} = a_y \\ \frac{dv_z}{dt} = -\frac{\partial \psi}{\partial z} = a_z \end{cases} \tag{2.3}$$

where (v_x, v_y, v_z) and (a_x, a_y, a_z) are the velocities and accelerations in respective direction. This system of equations can be solved numerically by discretizing and numerically integrating the six equations with respect to time, using e.g. the Runge-Kutta method (note that this can be done using the three original equations as well, however, for clarity the system of six first-order ODE's were used in this project).

This method of numerically solving the ODE's (the Euler method) uses the previous step's position and speed of the object to calculate the next step, and so each step's solution is based on the previously calculated step. This requires the initial conditions of the object (i.e. the initial three-dimensional position and speed, in total six vector composites), to be known in order to be able to start the integration.

A closer look at the three equations in (2.3) also states that the acceleration of an object in a gravitational potential is independent of the mass of the object. This enables the use of tracer particles in the simulation, which was used in the integration of the cluster orbit (see section 3.3.1).

2.3 The N-body Equation

The central equation of this project is the N-body equation;

$$\bar{F}_i = -\sum_{j \neq i} G \frac{m_i m_j (\bar{r}_i - \bar{r}_j)}{|\bar{r}_i - \bar{r}_j|^3} - \bar{\nabla} \cdot \phi_{ext}(\bar{r}_i), \tag{2.4}$$

where $\bar{F}_i$ is the force exerted on the star i, G is the gravitational constant, m_i and m_j are the masses of the different stars, $\bar{r}_i$ and $\bar{r}_j$ are the positions of the different stars, and $\bar{\nabla} \cdot \phi_{ext}(\bar{r}_i)$ is the gradient of the potential at position $\bar{r}_i$.

The N-body equation is divided into two parts, and gives the total force exerted on a star from these two.

2.3.1 Newton's Law of Universal Gravity

The first part of the equation;

$$\bar{F}_i = -\sum_{j \neq i} G \frac{m_i m_j (\bar{r}_i - \bar{r}_j)}{|\bar{r}_i - \bar{r}_j|^3}, \tag{2.5}$$

calculates the force exerted on star i from all other stars present in the N-body calculation. This is done by summing up the force exchanged through Newton's law of universal gravity between the star i and all the other stars.

Newton's law of universal gravity states that the gravitational force exchanged between two objects is proportional to the masses of the objects divided by the distance between their centre of gravity squared.

2.3.2 Gradient of the Potential

The second part of the equation is the gradient of the external potential. In order to be able to calculate the gravitational forces exerted on a cluster star by for example gas in the cluster, or the rest of the Milky Way, the gravitational potential of the cluster (or the galaxy) must first be established. The gravitational potential is determined by the mass distribution, and can be calculated using Poisson's equation for gravity,

$$\nabla^2\phi = 4\pi G\rho, \tag{2.6}$$

where ϕ is the gravitational potential, G is the Newton's constant of gravity, and ρ is the density. This states that the gravitational potential is uniquely determined by the density of the cluster (or galaxy), which correlates to the mass distribution. The force exerted on a body can then be calculated using the gravitational potential through

$$\bar{F} = \nabla\phi, \tag{2.7}$$

where $\nabla\phi$ is the gradient of the potential, and $\bar{F}$ is the resulting force.

The mass distribution of the galaxy can be determined by e.g. rotational velocity measurements of the Milky Way, producing a rotation curve. However, this method has a great uncertainty when measuring the density of the Milky Way at a radius of ~ 8 kpc or greater from the galactic centre (outside the galactic orbit of the Sun), since the rotational velocity cannot be uniquely determined.

2.4 Tidal radius

The distance from a cluster at which an object is no longer gravitationally dominated by the cluster is called the tidal radius r_t of the cluster. It is defined as (King 1962); (Perryman et al. 1997b)

$$r_t = \left[\frac{GM_C}{4A(A-B)}\right]^{1/3}, \tag{2.8}$$

where M_C is the mass of the cluster, and A and B are the experimentally determined Oort's constants which describe the rotation curve of the Milky Way in the solar neighbourhood. This gives us some sense of which stars in the neighbourhood of the cluster are members, and will in this project be used to quantify the number of bound stars throughout the integration time span. The tidal radius of the Hyades is calculated in Perryman et al. (1997b), where it is estimated to be $r_t \sim 10$ pc. This value will be used in this project as well.

Chapter 3

Method

This project consists of two major parts - combining an N-body simulation and a simulation in a galactic potential, and running numerical experiments using the code to investigate the stability of open clusters.

Usually when working with an N-body simulation, the force from the Milky Way is taken into account by introducing a small perturbation into the N-body calculation. This is where this project separates itself a little; instead of using a perturbation, it uses a second, "outer" integration that calculates the orbit of the mean of the cluster in a potential that represents the Milky Way, thus taking the force into account this way instead. This means two parallel integration loops instead of the usual one with only a small addition to running times, with the hope that it will have some interesting applications and be more true to the nature of cluster behaviour.

3.1 Initial Conditions

First of all, in order to have a practical example to work with when constructing the simulation, the cluster to be investigated was chosen to be the Hyades open cluster. The decision to use this cluster was based on the amount of astrometric data and the accuracy of the data of the cluster, due to its vicinity to the Sun. Next, the decision had to be made of which stars in the cluster were to be included in the N-body part of the simulation. As a reference, the table of stars in the Hyades open cluster in van Leeuwen et al. (2017) was used (which uses data from GDR1), and the criteria used was all stars with a Henry-Draper ID (HD) and a Gaia magnitude of $G \leq 8$. An extract of the table in van Leeuwen et al. (2017) of the included stars can be found in table A.1. This data from GDR1 was used throughout the project, even after GDR2 became available in April of 2018, since the focus of the project at this point was to finish.

In order to be able to use the Hyades and the selected stars within it in a simulation,

the individual initial conditions of all the selected stars, as well as the initial conditions of the mean of the cluster need to be known. This means that the initial three-dimensional position and velocity of each star, as well as of the mean of the cluster, have to be taken from a source. For this purpose, the astrometric data provided in A.1 is not enough; the table provides enough information in order for the positions of the stars to be determined (α, δ, and π), but provides no information about the velocity of each star. Thankfully, GDR1 provides us with the two proper motion vectors μ_α and μ_δ. The third and final velocity-component, the radial velocity v_r, was taken from the SIMBAD database by cross-referencing using the ID's of the stars, thus completing the initial conditions for all individual stars in the Hyades open cluster. The initial conditions can be found in table A.2, and were transformed into a galactocentric carthesian coordinate system in the Python script for ease of handling and understanding.

In van Leeuwen et al. (2017) the mean position and mean velocity of the Hyades is estimated by starting with the cluster centre and parallax derived in van Leeuwen (2009) and applying selection steps to the 285 stars in GDR1 TGAS that are likely to be within 16 pc of the assumed cluster centre, limiting the amount of stars believed to be actual members of the cluster. The initial conditions of the mean of the Hyades cluster were taken from the final 103 stars of the selection process, as stated in van Leeuwen et al. (2017).

3.2 Potentials

3.2.1 The Milky Way Potential

In this project, a simple Milky Way potential taken from "Dynamical Astronomy, Lecture Notes for ASTM13" by Lindegren (2014), originally used by Paczynski (1990), is being used.

It consists of three superpositioned sub-potentials; one for the bulge, one for the disc and one for the halo. For the bulge and the disc potentials (ψ_b and ψ_d), a Miyamoto-Nagai potential is used, which in cylindrical coordinates has the form

$$\psi_{MN}(R,z) = -\frac{GM}{\sqrt{R^2 + (a + \sqrt{z^2 + b^2})^2}}, \tag{3.1}$$

where G is the gravitational constant, M is the total mass of the system, and a and b determine the shape of the potential and have dimensions length.

The spherically symmetric potential used for the halo potential ψ_h has the form

$$\psi_h(r) = \frac{GM_c}{r_c}\left[\frac{1}{2}\ln\left(1 + \frac{r^2}{r_c^2}\right) + \frac{r_c}{r}\arctan\left(\frac{r}{r_c}\right)\right], \tag{3.2}$$

where M_c and r_c are two additional parameters related to the core of the potential.

The total Milky Way potential can then be calculated by adding the three potentials together;

$$\psi_{MW}(\mathbf{r}) = \psi_s(R, z) + \psi_d(R, z) + \psi_h(r) \tag{3.3}$$

The parameter values used for the total Milky Way potential can be found in table 3.1. The potential was tested by initiating an orbit that closely resembles the Sun's (radial velocity of 220 km/s and a distance of 8 kpc from the centre of the Milky Way, slightly off the centre of the disc in height to check the derivative perpendicular to the disc), and making sure that it was stable (roughly circular) and bobbed up and down over the disc.

$a_s = 0$	$b_s = 277$ pc	$M_s = 1.12 \cdot 10^{10}\ M_\odot$
$a_d = 3700$ pc	$b_d = 200$ pc	$M_d = 8.07 \cdot 10^{10}\ M_\odot$
	$r_c = 6000$ pc	$M_c = 5.0 \cdot 10^{10}\ M_\odot$

Table 3.1: Table of the parameter values used in the Milky Way-potential (eq. 3.3).

This potential is used for the Milky Way throughout the project.

3.2.2 The Plummer Model - The Hyades Cluster Potential

Since the total mass of the cluster cannot be accounted for by astrometric measurements of individual stars, the remainder of the cluster mass is represented by a gravitational potential. In this paper, the Plummer model was used for this purpose, as it is a simple potential model suitable for N-body calculations. The Plummer potential model can be written as

$$\psi_P(r) = -\frac{GM}{\sqrt{r^2 + a^2}}, \tag{3.4}$$

where G is the gravitational constant, M is the mass of the cluster, and a is the so called Plummer radius, which is a measure of the cluster core size.

In order for the simulated cluster to have the correct mass, the mass of the Plummer potential is initially set to the astrometrically estimated mass of the cluster ($\sim 400 M_\odot$, Perryman et al. (1997b)), with the combined mass of the individually simulated stars in the N-body simulation is subtracted from the potential mass. The mass of the cluster potential is then reduced as more N-body stars are migrating out of the cluster, simulating the cluster dissolving. This is done by fitting an exponentially decreasing function on the form of

$$M(t) \propto e^{-t} \cdot M_0 \tag{3.5}$$

to the initial and final estimated mass of the cluster[1], where $M(t)$ is the mass of the cluster as a function of time and M_0 is the initial mass of the cluster.

It is worth mentioning here, that as the field of astrometry advances (most current advances being the Gaia mission data releases), more accurate astrometric data becomes available. This means that more stars in nearby clusters can be included in the N-body part of the simulation, and thus the potential part of the simulation will be reduced. However, since clusters also contain large amounts of gas and dark bodies that can't be measured astrometrically, the potential will still have a high significance for the accuracy of the simulation, and so can never be completely removed from the simulation.

3.2.3 Differentiating the Potentials

In order to calculate the acceleration, and thereby the force exerted on an object by the potentials (according to section 2.2), the derivatives of the potentials with respect to position need to calculated. They are as follows for the mentioned potentials;

$$\frac{d\psi_{MN}}{d\bar{r}} = \begin{cases} \dfrac{d\psi_{MN}}{dR} = \dfrac{GMR}{u^3} \\ \dfrac{d\psi_{MN}}{dz} = \dfrac{GMz\ (1 + a/s)}{u^3} \end{cases} \quad \text{where} \quad \begin{cases} s = \sqrt{z^2 + b^2} \\ u = \sqrt{R^2 + (a+s)^2} \end{cases} \tag{3.6}$$

$$\frac{d\psi_h}{d\bar{r}} = \frac{d\psi_h}{r} = \frac{A}{r_c} \cdot \frac{1 - \arctan(u)/u}{u} \quad \text{where} \quad \begin{cases} A = \dfrac{GM_c}{rc} \\ u = \dfrac{|r|}{r_c} \end{cases}, \tag{3.7}$$

where the arctan-term was substituted with its Taylor expansion in the script for $u < 10^{-4}$, in order to not divide by zero for small r.

[1]The estimation of the final mass of the cluster was based on the simulated stars' to potential mass-fraction remaining constant, and observing approximately five N-body stars left in the cluster when running the N-body simulation for 100 Myr without decreasing mass potential. Since the amount of stars left in the cluster when running the N-body simulation for 100 Myr with a decreasing potential mass was roughly the same as before (around five), the method of final mass estimation of the cluster was assumed to be okay.

These are the equations used to calculate the acceleration due to the gravitational potentials throughout the project.

3.3 Integrating the Hyades open cluster

The code was written in Python 3.5 and consists of two parallel integration-loops; the "outer" loop, which integrates the orbit of the cluster in the Milky Way using the initial conditions of the mean of the Hyades open cluster, and the "inner" loop, integrating the individual orbits of the 32 stars in the N-body simulation.

The two integrations are done in parallel with the same time-step. In each time-step, the new mean position of the cluster is first calculated. The inner integration is then done using the updated position of the cluster, and a new time-step is initiated. See figure 3.1 for more details.

The initial thought was to have multiple intermediate time-steps in the inner N-body integration in the span of one outer Cluster Orbit integration time-step, in order to increase the precision of the inner N-body simulation while still keeping the code time-efficient[2]. However, the inner N-body integration is what takes up the vast majority of the time it takes to calculate one time-step, since it handles a lot more objects and (as will be explained in section 3.3.2) their individual force-exchange with all other bodies in the N-body simulation. Since the Hyades cluster orbit integration is just one more calculation, using the same time-step for both integrations would mean higher precision for the cluster orbit at a very low extra computational cost. See figure 3.1 for clarification.

3.3.1 The Cluster Orbit

The cluster orbit integration calculates (as the name states) the orbit of the cluster in the Milky Way, with the cluster being initiated as a test particle in the Milky Way Potential (see section 3.2.1) with the initial conditions from van Leeuwen et al. (2017) (see section 3.1). The integration is done using the Dormand-Prince method of solving ODE's (a variant of the Runge-Kutta method), which facilitates adaptive stepsize integration.

It is possible to initiate the cluster as a massless test particle due to the fact that the only force taken into account as acting on the cluster as a whole is from the Milky Way, which is accounted for using a potential. Since the acceleration in a gravitational potential is independent of the mass of the object, we do not need to introduce a total mass estimate for the cluster. The use of a massless test particle also means that all the stars in the

[2]Side note: This is also why the cluster orbit integration is called the "outer" loop and the N-body integration the "inner" loop; since multiple steps of the N-body had to be integrated in the span of one time-step of the cluster orbit integration in the first method, the N-body integrator had to be inside the cluster orbit integrator in the code.

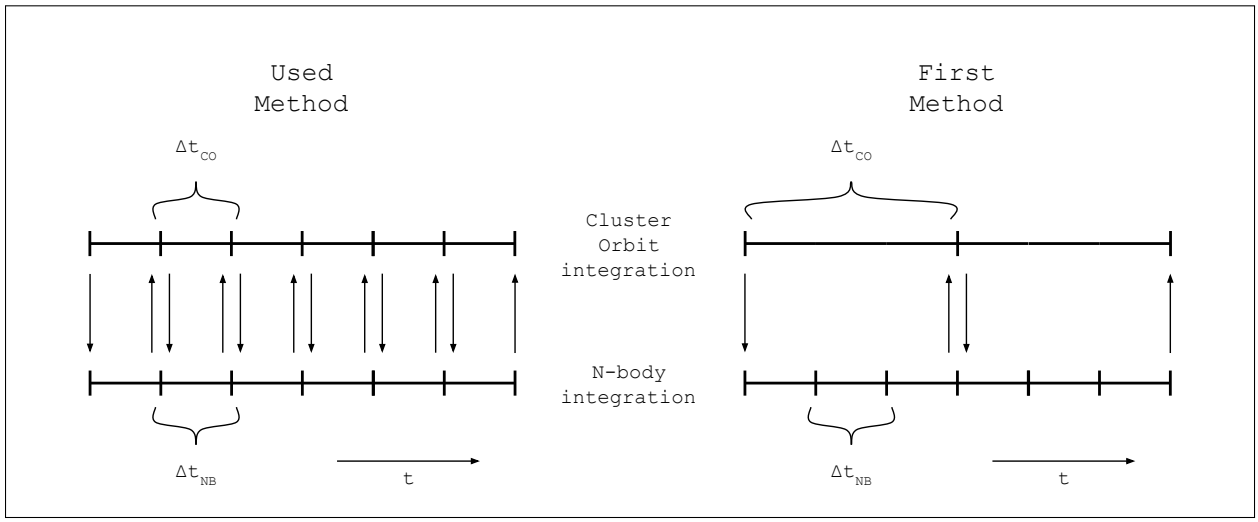

Figure 3.1: Image comparing the used method (left hand side) with the first method (right hand side), where Δt_{CO} and Δt_{NB} are time-steps in the Cluster Orbit and N-body integration respectively. In the first method, several intermediate integration steps were calculated in the span of one orbit integration-step with the intention to save running time in the orbit integration, since the precision of the cluster orbit integration did not need to be as high. However, since the orbit integration only contains one calculation and each step in the N-body contains hundreds, the cluster orbit integration was eventually set to the same time-step size as the N-body integration. This gives a higher accuracy in the cluster orbit integration at a very low cost in extra running time.

Hyades open cluster are treated as one body in the cluster orbit integration, and thus the force exerted on each individual star by the rest of the Milky Way is already accounted for before the N-body integration is done. Although this is an approximation it is a reasonable one to make, since the force exerted on a Hyades cluster star is approximately constant with respect to position in the cluster, due to the gravitational potential of the Milky Way being almost constant, and thus $\nabla\psi_{Galactic}(x, y, z) \sim 0$ over the cluster.

3.3.2 The N-body Orbits

The N-body integration calculates the orbits of the 32 individual stars, relative to the cluster centre. In other words, the N-body integration is done in the local frame of the cluster, and not in the galactocentric frame. The transformation is a simple one, and simply involves subtracting the mean vector of the cluster from the individual stars' vectors. The result is the stars' vectors in the local carthesian coordinate frame of the cluster.

The included stars have for simplicities sake all been given the same mass, 1.25 $M_{\odot}$, based on an average taken from Perryman et al. (1997b). Their initial conditions have been taken

from GDR1, with complementary radial velocities taken from the SIMBAD database (for more information about the initial conditions, see the section on Initial Conditions).

Three forces are taken into account that affect the integrated orbits of the stars in this N-body simulation;

The N-body force

The first force is what gives this part of the simulation its name; The N-body force. It calculates the force exerted on a given star by all other stars in the N-body simulation. This means that there are $n(n-1)/2 = 496$ calculations in each step[3].

The force exerted on a star with index i by any other star j follows Newtons law of gravitation as described in equation 2.5;

$$F_{ij} = G\frac{m_i m_j}{r_{ij}^2}, \tag{3.8}$$

where G is Newtons constant of gravitation, m_i and m_j are the respective masses of the stars, and r_{ij} is the distance between the two stars. This explains why we need to give the stars masses, in order for the N-body force exerted between the objects to be non-zero.

Gravitation is linear, and so the forces exerted on a given star by all other stars in the simulation can therefore simply be summed up to give the resulting acceleration on the star. By calculating the forces exerted on a given star and repeating this for all stars in the simulation, the forces mediated between the simulated stars has been accounted for. The force exerted on the star with index i from all other stars in the N-body calculation thus becomes (according to 2.5)

$$F_i = \sum_{j \neq i} G\frac{m_i m_j}{r_{ij}^2}. \tag{3.9}$$

The inclusion of star - star interactions results in more accurate dynamics, specifically when it comes to ejection of stars from the cluster. More sporadic movements and shifts in orbits due to N-body calculations closer resembles the true nature of cluster dynamics, since without them cluster migrations can only occur through the stars' interaction with the potentials in the simulation.

[3]This is the basis for why the time-step in the cluster orbit- and N-body integrations were set to the same value, see section 3.3 for reference.

The Cluster potential

The second force taken into account is the force from the Cluster potential, and for this the Plummer model is used (see section 3.2.2). It represents all the mass of the cluster that was not included in the N-body force calculation. This includes stars, gas and other matter, which exerts a force on the stars in the N-body simulation due to its mass, but can or was not included in the N-body calculation. Gas, for instance, is best approximated as a potential and not point-like particle, and since this is a simulation of an open cluster, which contain a lot of gas, the potential represents most of the cluster's mass.

As discussed in section 3.2.2, because of the high amount of gas and (to us) unobservable stars, the presence of a potential will always be true in an N-body simulation of this size, even as better observing methods become available and technology improves. However, more stars will be able to be included into the N-body calculation, and so the Cluster potential-part of the simulation will gradually decrease.

In order for the Cluster potential to be as accurate as possible, the mass of the potential needs to be reduced gradually as the cluster dissolves. The method of how this is done can be found in detail in section 3.2.2.

The Milky Way potential

The third and final force is the force exerted on each star by the rest of the Milky Way. Using the approximation that the gravitational potential is roughly constant throughout the volume of the cluster (due to the small volume of the cluster in comparison to the size of the Milky Way), and thus the force exerted on each star from the Milky Way being approximately equal, we can treat all the individual stars as one body. Thus, the force exerted on each individual star is accounted for in the Cluster Orbit integration.

3.3.3 The total force on a star

The total force on a star i when adding the two forces thus becomes, according to 2.4;

$$\bar{F}_i = -\sum_{j \neq i} G \frac{m_i m_j (\bar{r}_i - \bar{r}_j)}{|\bar{r}_i - \bar{r}_j|^3} - \bar{\nabla} \cdot \phi_{Cluster}(\bar{r}_i), \tag{3.10}$$

where $\phi_{Cluster}$ is the cluster potential.

Chapter 4

Results

The Results consist of three sections, and are used to demonstrate that both parts of the simulation works as intended. Results include analysis of the Hyades membership of some high velocity stars in the simulation, and results attempting to quantify the dissolution of the Hyades.

Throughout this chapter, the term "Base Run" will be used. This refers to integrating the Hyades open cluster orbit, as well as the internal N-body orbits, for a duration of 100 Myr, without any cluster collisions enabled. The Hyades orbit is thus integrated in the potential of the Milky Way, and the stars inside the cluster are integrated in the cluster potential in combination with the N-body interaction.

4.1 The Simulation

First, in order to find an optimal time resolution for the integration and to test if the integration of a massless test particle in a gravitational potential worked as intended, a sequence of Base runs (100 Myr integration without cluster collision) were initiated with varying resolutions (varying the time-step used). At a resolution of 100 000 years per time-step, the difference in results compared to higher resolution runs were negligible, and compared to lower resolutions there was a very small difference, and so this resolution was used. Coupled with the relative tolerance-parameter in the integrator used, making sure that each time-step is sub-divided into smaller time-steps if required for smoothness (for instance at high accelerations), this resolution was deemed satisfactory[1].

After the time resolution of the integration was established, a 500 Myr integration of the Hyades open cluster's orbit in the Milky Way was done. Figure 4.1 shows two of the

[1]The effect of the relative tolerance was also tested in a similar way to the step-resolution, but had less impact on the outcome of the integration. It was eventually set to 10^{-6}.

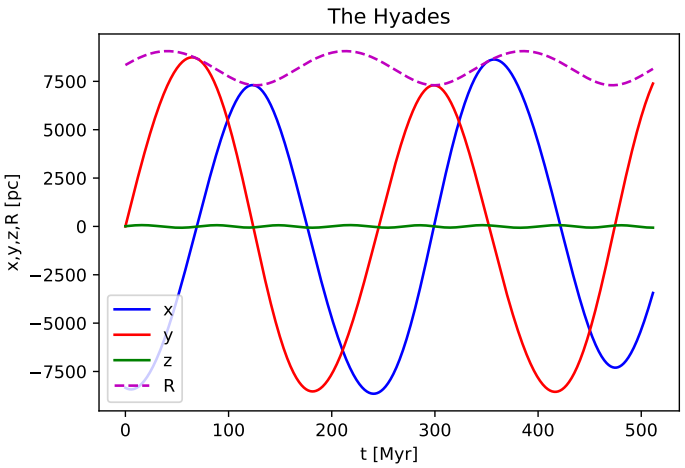

(a) x-position (blue), y-position (red), z-position (green), and radius $R = \sqrt{x^2 + y^2}$ (magenta) on the vertical axis in parsec, against time t on the horizontal axis in Myr. The position is relative to the galactic centre.

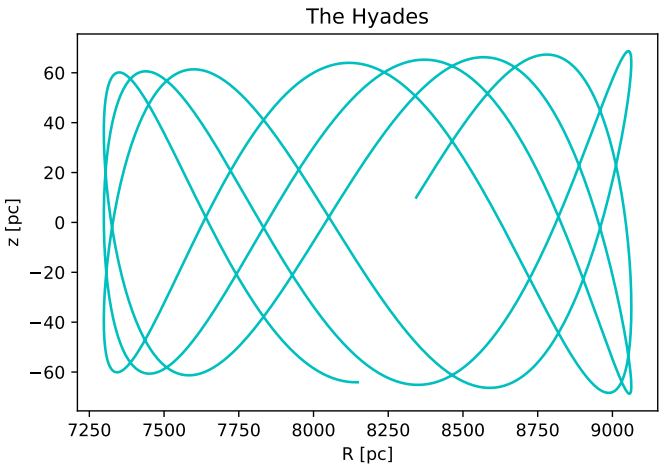

(b) Height z relative to the galactic plane in parsec (vertical axis), against radius $R = \sqrt{x^2 + y^2}$, also in parsec (horizontal axis).

Figure 4.1: (a) Position against time- and (b) height against radius-plots of the Hyades open cluster in the Milky Way, over a timespan of 500 Myr. The plots are made in a galactocentric coordinate system.

resulting plots from the run; Figure 4.1a shows each coordinate (x, y, z), as well as the radius = $\sqrt{x^2 + y^2}$ of the Hyades as a function of time, while figure 4.1b shows the radius R as a function of height z. All distances are expressed in the unit parsec, and time in Myr (Million years). The Hyades seems to be in a stable orbit around the galactic centre, with harmonically oscillating x- and y-values with slightly different wave amplitudes. This difference in amplitude leads to the radius R oscillating slightly as a function of time, which means a slightly elliptical orbit. The height above or below the galactic plane also oscillates with an amplitude of about $\pm$60 pc, with a periodical of $\sim$80-85 Myr. The height oscillation can better be seen in 4.1b, where the eccentricity can also be seen in the distance span of the plot. For a more detailed plot of the height oscillation as a function of time, and the x-y plane orbit, see Appendix C.

Similarly, in order to test that the N-body interaction was working correctly, the N-body was tested on its own as well as with the potentials. The most interesting and telling test was to plot the local velocities of the stars in the N-body simulation relative to the cluster centre as a function of time in a Vanilla run, an example of which can be seen in figure 4.2. Figure 4.2 shows the velocity-time plot of one of the more interesting stars in this test, HD27808. In the plots, the difference when the N-body equation was used (b) and when it was not (a) can be clearly discerned; both velocity curves have an exponentially decreasing velocity, but when the N-body equation is used, a "bump" in the velocity-curve

can be noted at $t = 11.6$ Myr, which is caused by an N-body interaction with HD26784, another star in the simulation. The closest approach between the stars was 0.36 pc, which corresponds to an acceleration of ~ 0.04 km/s^2. This is a good indication of a working N-body interaction.

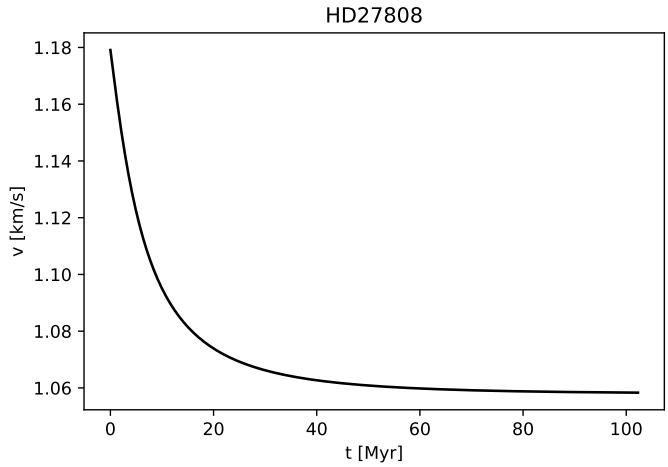

(a) Velocity-time plot of the star HD27808 in a simulation without N-body incorporated, with velocity v in km/s on the vertical axis, and time t in Myr on the horizontal axis.

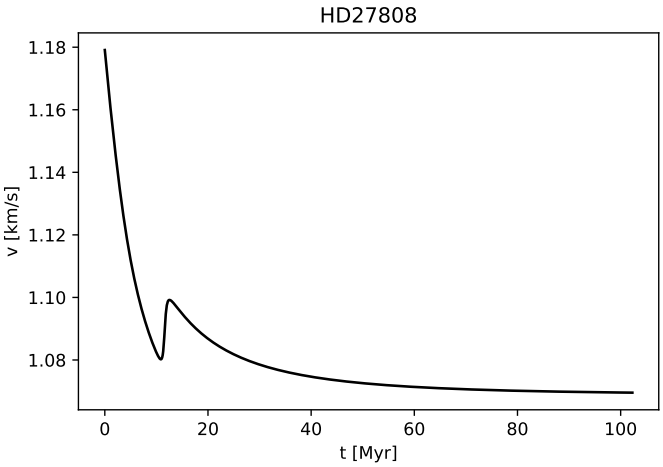

(b) Velocity-time plot of the star HD27808 in a simulation with the N-body equation incorporated, with velocity v in km/s on the vertical axis, and time t in Myr on the horizontal axis.

Figure 4.2: Comparison of velocity versus time plots of the star HD27808, without (left hand side) and with (right hand side) the N-body equation implemented. The velocity is measured in km/s relative to the cluster centre. The bump at $t = 11.6$ Myr in (b) is due to a close encounter with the star HD26784, where the two stars got as close as 0.36 pc, which corresponds to a maximum acceleration during the encounter of 0.04 km/s^2.

4.2 High Velocity Stars

Some of the stars included in the N-body simulation (in particular one, HD31236) appears to (with the initial conditions used) not be in stable orbits in the Hyades, but instead to be merely passing within the tidal radius of the cluster with a high local velocity. This could either be due to the stars not really being a member of the Hyades, or due to gravitational interactions with other objects in (relative) recent history, accelerating them out of the cluster. This was tested further by integrating the orbits backwards in time, to ensure that the stars were not in highly elliptical orbits, and that they had not interacted with other stars included in the N-body. However, due to not being able to include all of the cluster mass in an N-body calculation (such as gas, dark bodies, etc.), as well as not having taken the formal errors of the initial condition into account, this result is merely indicative.

Two examples of individual star orbit plots can be seen in figures 4.3 and 4.4 respectively. The two figures shows the same parameters as figure 4.1 did for the Hyades orbit in the Milky Way, but for the most bound (HD28992, figure 4.3) and most unbound (HD31236, figure 4.4) star in the simulation, in the local frame of the Hyades. The time frame of the integration is 200 Myr. The two plots for HD28992 indicate that the star starts of in a stable orbit with harmonically oscillating x-, y-, z- and R-values, and does not seem to become unbound until $t \sim 150$ Myr, while all of the plotted values for HD31236 seem to be linear. The difference in velocity relative to the Hyades centre can be seen in figure 4.5, where the local velocity of both stars has been plotted as a function of time (cropped at 100 Myr for HD31236). In this figure, the velocity of HD28992 appears to be oscillating at a velocity of ~ 0.3 km/s, while HD31236 does not oscillate, but exponentially increases until it peaks at a velocity of ~ 6.5 km/s within the first 5 Myr and then exponentially decreases.

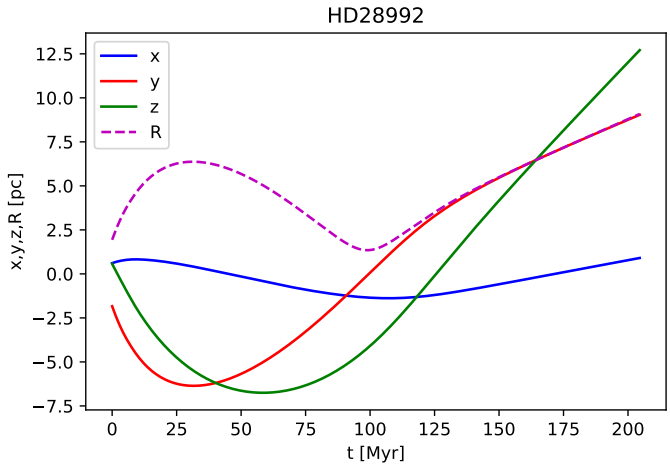

(a) x-, y-, and z-values (in blue, red and green respectively), as well as radius $R = \sqrt{x^2 + y^2}$ (dashed magenta line), expressed in parsec from centre of the Hyades open cluster, as a function of time t. The star appears to have a stable orbit, but becomes less bound towards the end of the simulation, which is due to the decreasing mass of the potential.

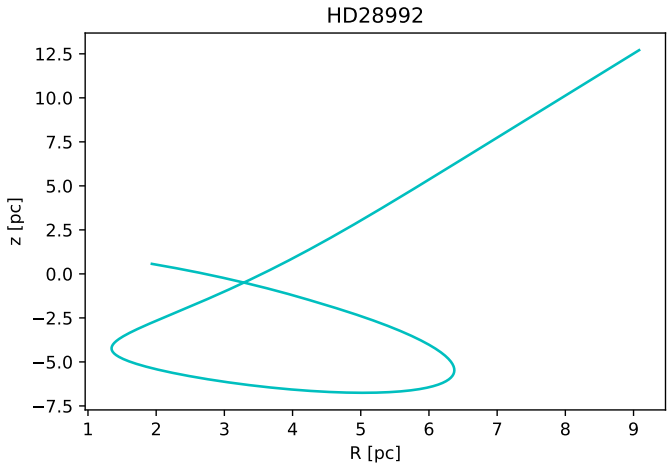

(b) Radius $R = \sqrt{x^2 + y^2}$ (horizontal axis) against height z (vertical axis) of one of the most bound stars in the simulation, HD28992. Both axis are in parsec.

Figure 4.3: Position (x, y, z, R) against time t, as well as height z against two-dimensional radius R, of one of the most bound stars in the simulation, HD28992.

Figure 4.6 shows the two stars' respective distance r in parsec relative to the cluster centre as a function of time. In both plots in figure 4.6, the tidal radius of the Hyades is plotted as a threshold value. HD28992 (a) oscillates within the tidal radius for most of the simulation, while HD31236 appears to have a linear trajectory throughout the simulation, and barely makes it inside the volume gravitationally dominated by the Hyades. The distance R and

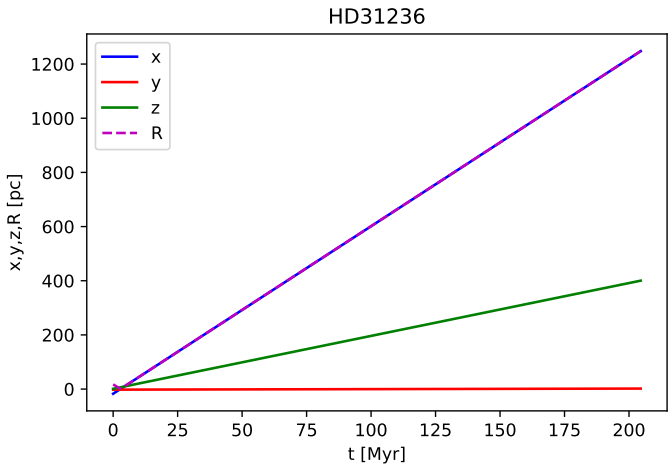

(a) x-, y-, and z-values (in blue, red and green respectively), as well as radius $R = \sqrt{x^2 + y^2}$ (dashed magenta line), as a function of time t. All four lines appear linear, which indicates that the star has not been affected very much at all by other stars or the cluster potential. Furthermore, the y coordinate appears almost constant at $y = 0$, which leads to the x- and z-lines coinciding.

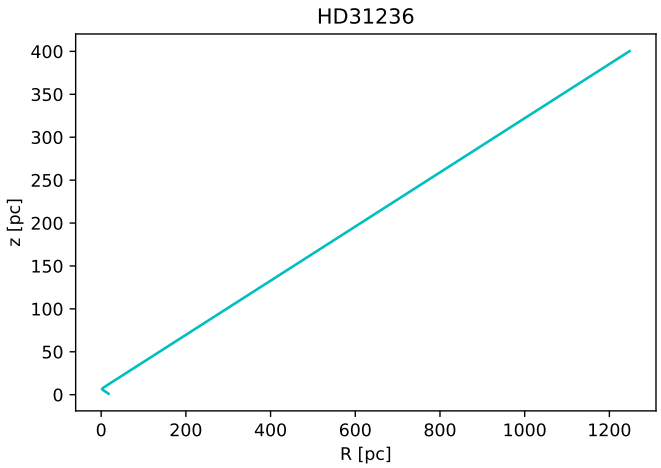

(b) Radius-to-height plot of HD31236, where $R = x^2 + y^2$ is the radius and z is the height. Both axis are in parsec. The data is indicative of the star not being a cluster member at all but that it is merely passing through the cluster, although this cannot be said with absolute certainty since the error of the astrometric data has not been taken into consideration in this project.

Figure 4.4: Position (x, y, z, R) against time t, as well as height z against two-dimensional radius R, of the star HD31236.

height z of HD31236 (figure 4.4) also appears linear as a function of time, which also indicates that no major gravitational interaction perpendicular to the direction of travel has occurred. The combination of the high relative speed of HD31236 and the absence of gravitational interactions between the star and the cluster indicates that the star is not an actual member of the Hyades open cluster, but is merely passing through. However, this can not be stated with certainty, as the formal errors of the initial conditions have not been taken into account, and a gravitational interaction within the cluster in history cannot be ruled out.

To rule out an highly elliptical orbit of HD28992, which would look similar to it leaving the cluster, a longer integration of 500 Myr was done, which confirmed that the star indeed becomes unbound. The reason for this is the mass decrease of the cluster potential, and not an N-body interaction, as this would show more clearly in the plot. Also, only a few stars remain within the tidal radius of the cluster at this point in time, and so the chance of a significant N-body interaction is quite low.

The plot of x-, y-, z- and R-values as a function of time, as well as radius R against height z, of the star HD31236 when integrated backwards in time can be found in Appendix C.

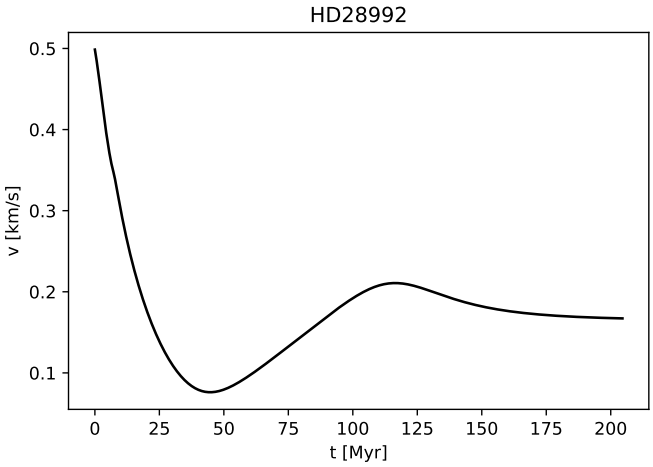

(a) The velocity v of the star HD28992 relative to the Hyades centre, as a function of time t. The velocity appears to oscillate like a dampened harmonic around $v \sim 0.2$ km/s, indicating that it is gravitationally bound. A slight perturbation can be seen at $t = 8.8$ Myr, which is due to a minor N-body interaction with HD28205.

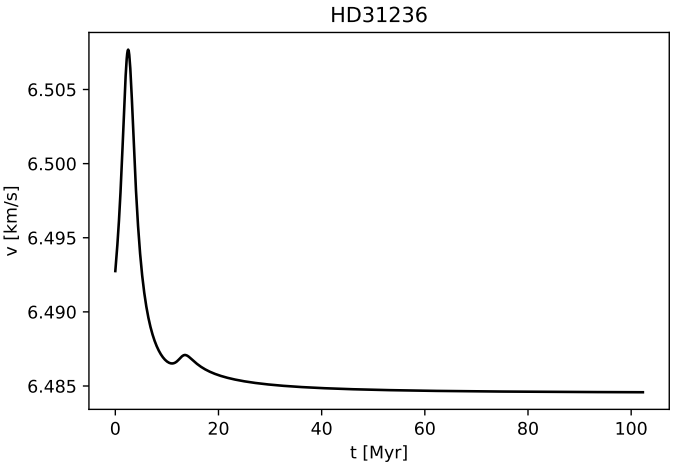

(b) The velocity v of the star HD31236 relative to the Hyades centre, as a function of time t (cropped at $t = 100$ Myr). In difference to figure 4.5a, the velocity does not seem to oscillate, but instead exponentially increase until it reaches its closest approach to the cluster centre (6.6 pc at time $t = 2.5$ Myr) at a velocity of $v \sim 6.5$ km/s, and then exponentially decrease. This is what would be expected of a star that is passing through the cluster at high speed. A perturbation in the velocity at $t = 13.1$ Myr can be seen, which is due to an encounter with the star HD28911 (2.3 pc distance at closest approach).

Figure 4.5: Comparison of velocity versus time plots of the stars HD28992 and HD31236. The velocity (vertical axis) is measured in km/s relative to the cluster centre, as a function of time t in Myr (horizontal axis). Comparing the two, it is apparent that HD31236 has a much higher velocity than HD31236.

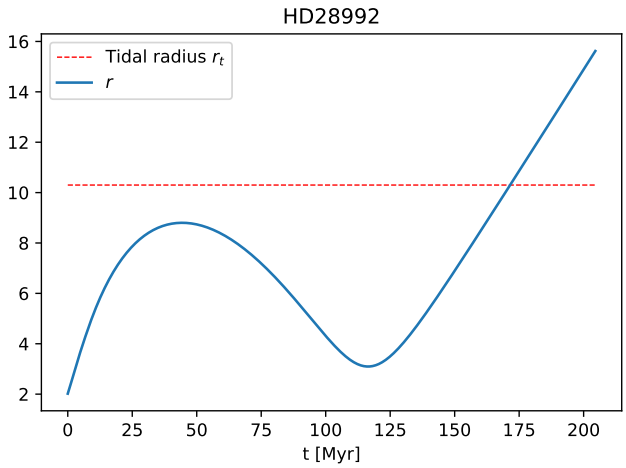

(a) Distance of HD28992 to the Hyades centre as a function of time. The distance appears to oscillate, indicating a gravitationally bound star, until the very end of the simulation. An integration with a time span of 500 Myr was done in order to rule out a highly elliptical orbit of HD28992, which confirms that the star becomes unbound, due to the mass decrease of the cluster potential.

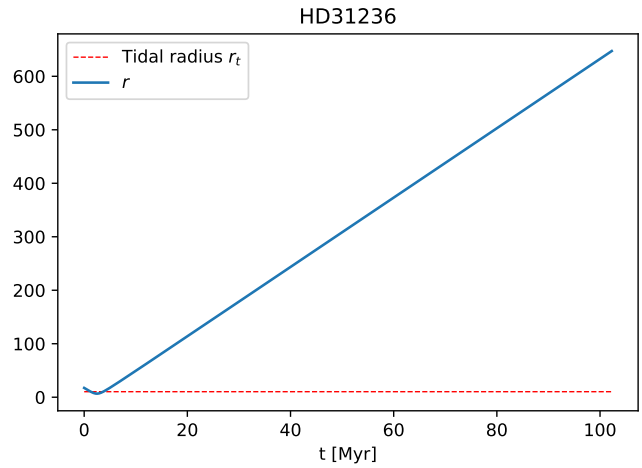

(b) Distance of HD31236 to the Hyades centre as a function of time (cropped at $t = 100$ Myr). Contrary to HD28992, the distance does not seem to oscillate with time, but instead be linear, indicating that no major interaction with another star or the cluster potential has occured. This in turn indicates a high relative velocity, which can be seen more clearly in figure 4.5. This all points towards that HD31236 is not a member of the Hyades open cluster, since it barely makes it inside the tidal radius of the cluster, and because of its high velocity relative to the Hyades.

Figure 4.6: Distance r from the cluster centre in parsec (vertical axis) for the two stars HD28992 (a) and HD31236 (b) as a function of time t in Myr (horizontal axis). The tidal radius r_t of the Hyades, taken from Perryman et al. (1997b), is marked as a dashed red line at $r_t \sim 10$ pc. HD28992 appears to stay bound for most of the 200 Myr-timespan of the simulation, only becoming unbound at $t \sim 90$ Myr, while HD31236 barely passes within the tidal radius of the cluster.

4.3 Dissolving Time of the Hyades

In order to compare the dissolution times of different runs, and thus be able to draw any conclusions about the impact of cluster collisions, some comparison value first has to be defined. For this, the number of gravitationally bound stars (stars located within the tidal radius of the Hyades, 10.3 pc) was plotted as a function of time, along with the two threshold values, 20% and 10% of the initial number of gravitationally bound stars. The Hyades was collided with other open clusters of the same radius as the Hyades at the time of $t \sim 0.9$ Myr, at a relative velocity of $v \sim 15$ km/s, varying the centre-to-centre distance at closest approach (0.3 pc, 0.7 pc and 1.7 pc), as well as densities ranging from $1\rho_H - 8\rho_H$ (where ρ_H is the density of the Hyades). Figure 4.7 shows the result from six of these runs; (a) - collisions with two different density clusters ($\rho_c = \rho_H$ and $\rho_C = 8\rho_H$) with a 0.3 pc separation at impact, (b) - same as (a) but with a 0.7 pc separation at impact, and (c) same as the previous two, but with a separation of 1.7 pc at impact.

It is clear when looking at figure 4.7 that the density of the oncoming cluster has a big effect on the outcome of these simulations. With both clusters having the same density we see no significant difference in dissolving time, and varying the centre-to-centre distance at impact matters little as well. However, as we start to increase the density of the oncoming cluster, we start to see differences in behaviour; overall the time it takes for the Hyades to drop below 10% of its original star population is decreased. Also, the effect of varying centre-to-centre distance becomes more apparent; the greatest dynamical change to the Hyades seems to occur when the off-set is at its greatest (1.7 pc), with smaller off-sets generating smaller differences in dissolving time. This of course does not extend to infinity; at a certain centre-to-centre distance the interaction will become weaker again, since the gravitational force scales as r^{-2}.

Plots similar to 4.7, but for densities $\rho_C = 2\rho_H$ and $\rho_C = 4\rho_H$, can be found in figure C.3 in the Appendix.

It should be remembered that the resolution of these results is quite low because of the low number of stars in the N-body, and so statistical fluctuations play a big role.

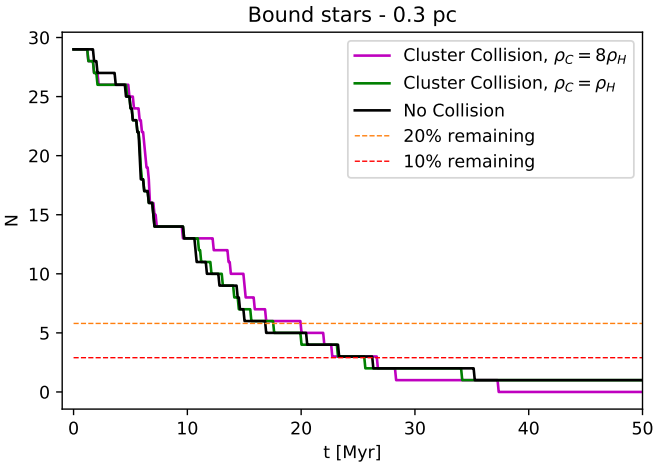

(a) Number of bound stars in The Hyades, when colliding with a cluster with a centre-to-centre distance of $r \sim 0.3$ pc at the time of impact, as a function of time.

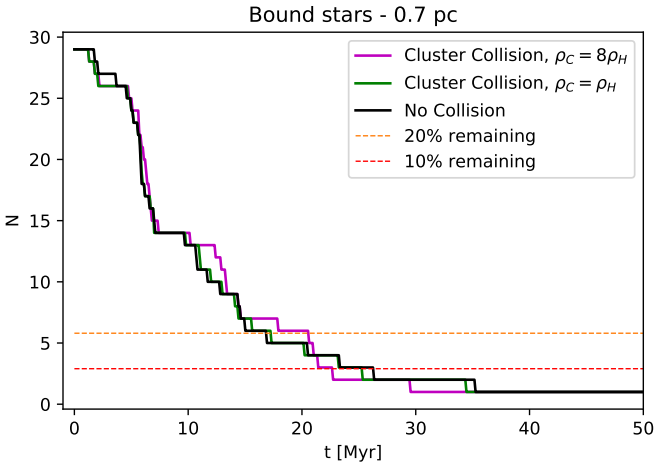

(b) Number of bound stars in The Hyades as a function of time, when colliding with a cluster. Here, the centre-to-centre distance is $r \sim 0.7$ pc at the time of impact.

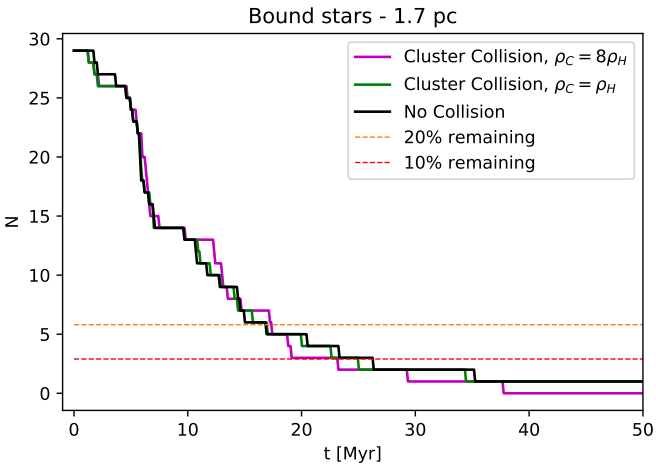

(c) Number of bound stars in The Hyades as a function of time, with a impact centre-to-centre distance of ~ 1.7 pc.

Figure 4.7: Number of bound stars N (stars within the tidal radius r_t) in the Hyades open cluster (vertical axis) as a function of time t in Myr (horizontal axis). No cluster collision in black, collision with a cluster of the same density and volume in green ($\rho_C = \rho_H$, $400M\odot$), and collision with a cluster with a density of $\rho_C = 8\rho_H$ ($3200M\odot$). The time of the collision is 0.9 Myr into the simulation, and the relative velocity of the clusters is $v \sim 15$ km/s. Threshold values for 20% and 10% of the initial number of bound stars marked as dashed orange and dashed red line respectively. If the colliding clusters are of the same density there seems to be little effect on dissolving time, no matter the distance at impact. However, increasing the density of the oncoming cluster to eight times that of the Hyades, we start to see the effects of the off-set at impact. The plots are cropped at $t = 50$ Myr, since all N remain constant to the end of the simulation (100 Myr) after this point.

Chapter 5

Discussion

Two integrations - is it worth it?

The core idea of this project was the implementation of a double integrator; one for the cluster in the Milky Way potential, and one for the local motions of the stars inside the cluster, something that is not commonly done when looking into local motions in a cluster. This of course raises the question, is it worth doing?

The most common way of doing a simulation of local motions of stars inside a cluster is, as discussed earlier, to do a local simulation (cluster potential and N-body) with a force perturbation representing the gravitational force exerted by the Milky Way. This is in comparison with the model used in this project a little bit more simplistic, but eases handling of a lot of things. For instance, colliding two clusters in such a model (if what one is interested in is merely the effect on one of the clusters, as in this project) simply involves tracing the wanted trajectory of the colliding cluster and initiating a potential in said trajectory. Since there is no "outer" (Milky Way) potential to take into account, the trajectory (for all intents and purposes) will be linear, and thus much easier to handle.

However, such a simulation is after all an approximation. A perturbation representing the gravitational forces from outside the cluster might not give the same result as a more rigorous integration of the cluster, where the Milky Way orbit of the cluster is traced out as well. This was the thought behind the project; to create such a simulation and investigate whether or not it is a viable method of integration.

As touched on in section 3, this method of integration has a very small impact on the running time compared to just one integration, since the cluster orbit integration only consists of one body in a potential. This, coupled with the fact that it is in fact a more complete picture of the cluster, makes it a very useful and versatile tool. Instead of having to calculate the position-specific perturbation in a cluster (caused by the outside mass distribution), the cluster can instead be integrated in the Milky Way potential in a separate integration. This in turn enables a great deal of flexibility, for instance initiating

new clusters of interest into the same simulation, or investigating the effect of the cluster orbit on the local motions of the stars inside the cluster.

On the membership of stars

One of the more unique and interesting stars in this simulation is HD31236. The reason for this is, with the initial conditions used in this project, the star starts by passing the centre of the Hyades at a high local speed, and seems to be almost unaffected by the potential of the cluster or by other stars. This strongly suggests that, according to this simulation, HD31236 is not a member of the Hyades open cluster. Compare this result to those stated in table 2 in Perryman et al. (1997b), where the independent investigations by van Bueren, Pels et al., Schwan, and Perryman et al. respectively, all concluded that the star HD31236 (HIP22850, used in the table) is a member of the Hyades.

Among the 32 stars included in this N-body simulation, HD31236 is the only star which has such a high local speed and can be seen passing the cluster centre during the time span of the integration. Integrating the cluster backwards in time does not indicate that it is a member on a highly elliptical orbit, but instead supports the notion that the star is merely a drifting star passing through the Hyades. Indeed, almost all 32 stars in the simulation seem to be leaving the cluster within 20-30 Myr, but show signs of interaction with other stars in the simulation, or at least with the potential of the cluster. In order to establish the membership status of more stars in the cluster, more accurate data and further investigation is needed, something that GDR2 might enable.

Whether or not our results differ from the rest of these investigations because of different simulation techniques or because of the more accurate astrometric data of GDR1 being used in this project cannot be said for certain. Comparing the radial velocity used in Perryman et al. (1997b) (also in table 2) with the radial velocity used in this project[1], we can see a difference in radial velocity of $\sim$10%. This could potentially explain the different outcome of the simulations, or at least be a part of it.

However, that HD31236 is not a member of the Hyades cannot be claimed for certain, since the errors of the initial conditions have not been taken into account in this simulation. If the integration was done varying the initial conditions within the formal errors and this still resulted in the star leaving the cluster at such a high local speed with no signs of major interaction, the result might be linked to the different simulation technique. This is something that could be the subject of further investigation.

[1]The radial velocity used in this project is not taken from Gaia but from the SIMBAD database, but has nevertheless been updated since the time of publishing of the paper, 1997, and so the same point applies.

The effect of cluster interactions on dissolving time

Varying the mass of the cluster colliding with the Hyades in the simulation, as well as the centre-to-centre distance at the time of closest approach in the simulation (from here on called the impact distance), allows us to make some rough conclusions about the effects of cluster collisions. Analyzing the results in section 4.3, we see that a collision with a cluster of the same mass and density ($400M_{\odot}$, green line in figure 4.7) results in little to no difference in dissolving time, with the impact distance having little effect as well. However, as the density of the oncoming cluster is increased and the impact distance varied, we start to see some changes. For an oncoming cluster of eight times the density[2] (a mass of $3200M_{\odot}$, purple line in figure 4.7), we start to see the effect that the centre-to-centre distance at the time of impact has on dissolving time. At the smallest distance, 0.3 pc (figure 4.7a), we see that the cluster collision seem to have prolonged the dissolving time consistently up to the time at which the cluster stays above 20% of the original star count of the N-body. At the time at which the cluster has 10% of the starting count the rate of decay is approximately the same, with a steeper decline after that. Moving on to the medium impact distance, 0.7 pc in figure 4.7b, we see that this roughly follows the outline of the "No Collision" base run, but with a slightly steeper decent after half of the initial stars have become unbound. Finally, in figure 4.7c, with an impact distance of 1.7 pc, we can observe the same trend as in the previous plot, where the collision seems to have little effect on the first 15 or so stars to leave the cluster, but increase the rate of decay quite substantially after this point.

It is important to bear in mind that the resolution of the relevant plots in this section is based on only 32 stars, and so there is room for statistical errors in the conclusions made. I have tried to take this into account and draw safe conclusions based on the data I have produced, but higher resolution simulations need to be done if one is to rule out statistical errors. To this it should be added that, as the cluster dissolves and the N-body stars leave the cluster, the impact of the statistical errors becomes greater, which makes it harder to draw conclusions as time increases in the plots.

In conclusion, the cluster collisions seem to have at least some effect if the density of the oncoming cluster is larger than the density of the cluster in focus, and this effect seem to be more dramatical when the clusters impact slightly off-centre, tending towards shorter lifetimes for the cluster. As expected, the higher the density ratio between the clusters, the more dramatical the change. However, the more detailed effects of the impact distance require a higher resolution simulation to be able to discern, including more stars in the N-body simulation.

[2]Same volume, eight times the mass

Improvements

In order to improve on the simulation, a number of things can be done, ranging in amount of work. First of all, in order to get more certain results when it comes to membership of stars, one can include the errors of the initial conditions. This is something that should be quite easy to implement if done correctly from the start, but was not done in this project, since it was not the original goal to determine membership status.

Another small improvement which could be done in order to increase the accuracy of the N-body simulation is to calculate the individual masses of the stars in the simulation, using available astrophysical parameters. This would lead to more accurate interactions between stars, and becomes increasingly important as more stars are added into the N-body portion of the simulation, increasing the number of interactions.

One can also test the impact of other forms of gravitational potentials on the cluster. One example of this would be to test a more rigorous model of a spiral arm, which could be implemented into the potential of the Milky Way. By varying for instance the rotational speed of the spiral arm, one can investigate what speed is required in order to tear the cluster apart when the cluster enters the spiral arm.

As done in this project, the oncoming cluster density and the centre-to-centre distance at impact can be varied in order to investigate the effect, but to a greater extent in order to get a more complete image of the effects. However, one can also vary the relative velocity at impact, which in theory should lead to more dramatic changes, due to longer interaction times. In this project the relative velocity was kept roughly constant at $\sim$15 km/s, since changing a third variable (already varying closest distance and density) would involve a lot more analysis to be able to draw good conclusions.

Chapter 6

Conclusions

In this project, a double integration simulator was constructed, with the intention of being a more flexible and intuitive alternative to the perturbation method of simulating clusters in a galactic potential. In the outer integration, the cluster was treated as one body and integrated in a Milky Way potential, and after every outer integration step the inner local motions of the stars inside the cluster were integrated. The simulation was tested in various ways to ensure that it worked as intended. The N-body calculation was tested by comparing results from when it was enabled and disabled, and the potential derivatives were checked mathematically during the project. The resolution of the integration was also tested to make sure that the results were accurate.

Using the new simulation, the test subject of the project, the Hyades open cluster, was collided with clusters of varying densities and centre-to-centre distance at impact, in order to investigate the effect of collisions on dissolving time of the cluster. It was concluded that the collision had an insignificant effect if the colliding clusters had approximately the same density, but as the density of the oncoming cluster was increased, the effect became more dramatical. Overall, all collisions with clusters with a density of at least two times that of the Hyades seemed to shorten the lifetime of the open cluster, with the greatest of the three off-sets having the most dramatical effect on the dissolving time of the cluster, increasing the rate of decay substantially.

The results also indicated that in particular one of the stars included in the N-body simulation, considered to be a member of the cluster, had a very high local velocity and left the cluster very early in the simulation. This was investigated further, and the results indicated that this star is merely passing through the cluster, although to prove this, further investigation is required, taking the formal errors of the star's initial conditions into account.

Acknowledgements

My deepest gratitude to my partner Frida Ekstrand, for constant moral support and unwavering love.

To my dear friends and family; Thank you for your encouraging words, they do mean the world to me.

To my supervisor David Hobbs, thank you for your time, and for passing up on your coffee breaks to discuss the project with me.

This research has made use of the SIMBAD database, operated at CDS, Strasbourg, France.

Bibliography

Brown, A. G., Vallenari, A., Prusti, T., et al. 2016, Astronomy & Astrophysics, 595, A2

ESA. 2018, Gaia DR2, `https://www.cosmos.esa.int/web/gaia/dr2`, accessed 2018-12-14

Frommert, H. & Kronberg, C. 2001, The Messier Catalogue, `http://www.messier.seds.org/xtra/ngc/hyades.html`, accessed 2018-12-13

King, I. 1962, The Astronomical Journal, 67, 471

Lecar, M. 1972, Gravitational N-body Problem, Proceedings of Iau Colloquium No.10

Lindegren, L. 2014, Dynamical Astronomy, Lecture Notes for ASTM13

Perryman, M. et al. 1997a, star, 2, $2\pi 1$

Perryman, M. A., Brown, A., Lebreton, Y., et al. 1997b, arXiv preprint astro-ph/9707253

Prusti, T., De Bruijne, J., Brown, A. G., et al. 2016, Astronomy & Astrophysics, 595, A1

van Leeuwen, F. 2009, Astronomy & Astrophysics, 497, 209

van Leeuwen, F., Vallenari, A., Jordi, C., et al. 2017, Astronomy & Astrophysics, 601, A19

Appendix A

Tables

A

Table A.1: Extract from the table in van Leeuwen et al. (2017) of the stars in the Hyades open cluster chosen to be included in the N-body simulation of this project. The criteria was set to any star with a Henry-Draper ID and a Gaia magnitude of $G \leq 8$.

SourceId	HD	α [degr]	δ [degr]	G	dm
45367052352895360	25825	61.5677	15.6980	7.666	3.36
46975431705914112	26345	62.6770	18.4231	6.477	3.34
3304412597612195328	26767	63.6141	12.4353	7.840	3.39
52813460492850304	26737	63.6272	22.4517	6.925	3.92
149005266040519808	26736	63.6352	23.5747	7.851	3.27
3300934223858467072	26784	63.6436	10.7014	6.945	3.27
49365082792386816	26874	63.9273	20.8197	7.600	3.50
3312136494998639872	26911	63.9434	15.4006	6.199	3.32
47620260916592384	27149	64.5082	18.2567	7.313	3.35
49231663928585344	27524	65.3823	21.0397	6.661	3.42
47541096078933376	27534	65.3849	18.4174	6.670	3.39
3311024785663873920	27561	65.3954	14.4097	6.477	3.45
145373372976256512	27808	66.0613	21.7361	6.969	3.16
3313947699887831808	27848	66.0932	17.0788	6.828	3.51
3313662892016181504	27859	66.1185	16.8861	7.627	3.27
3312783557591565440	27991	66.4060	15.9409	6.297	3.38
145293177350363264	28033	66.5775	21.4703	7.201	3.37
3313689417734366720	28099	66.6676	16.7468	7.916	3.30
3312709374919349248	28205	66.9000	15.5891	7.247	3.37
3306922954457367936	28237	66.9424	11.7364	7.331	3.32
3314109912215994112	28344	67.2017	17.2853	7.671	3.32
3314212063714381056	28406	67.3769	17.8630	6.764	3.33
3305871821341047808	28608	67.7387	10.7517	6.886	3.36
3307815001984777088	28635	67.8727	13.9034	7.600	3.65
3307528029449757056	28911	68.4448	13.2518	6.489	3.32
3312575681175439616	28992	68.6476	15.5045	7.739	3.31
146677874804442240	29419	69.7142	23.1497	7.343	3.19
3405113740864365440	30589	72.3842	15.8886	7.550	3.40
3404812680839290368	30712	72.6413	15.0833	7.517	3.36
3405220084257276416	30738	72.7026	16.2103	7.135	3.48
3404850785786832512	30809	72.8470	15.4334	7.728	3.92
3408463506117452544	31236	73.7435	19.4853	6.278	3.99

Table A.2: The initial conditions of the 32 stars in table A.1. One star (*) indicates they were taken from GDR1, two stars (**) indicate they were taken from the SIMBAD database by cross-referencing ID's. They were later transformed into a galactocentric carthesian coordinate system in the code to facilitate integration and plotting.

SourceId	HD	α [degr]*	δ [degr]*	π [mas]*	μ_α [mas/yr]*	μ_δ [mas/yr]*	v_r [km/s]**
45367052352895360	25825	61.5677	15.6980	21.3420	118.9340	-19.6168	37.75
46975431705914112	26345	62.6770	18.4231	21.3141	121.5019	-30.9246	36.10
3304412597612195328	26767	63.6141	12.4353	20.9219	114.8247	-13.0578	38.323
52813460492850304	26737	63.6272	22.4517	15.6472	92.6914	-32.4949	38.4
149005266040519808	26736	63.6352	23.5747	22.1908	119.8210	-48.3050	37.50
3300934223858467072	26784	63.6436	10.7014	22.1838	119.5726	-5.5164	37.10
49365082792386816	26874	63.9273	20.8197	19.8695	109.6238	-35.1506	27.2
3312136494998639872	26911	63.9434	15.4006	21.8505	115.6340	-21.5155	36.4
47620260916592384	27149	64.5082	18.2567	21.2855	113.1573	-31.2975	38.00
49231663928585344	27524	65.3823	21.0397	20.8987	104.8388	-35.9854	37.1
47541096078933376	27534	65.3849	18.4174	20.4678	110.6104	-31.8652	37.0
3311024785663873920	27561	65.3954	14.4097	20.4476	104.2298	-19.1325	39.80
145373372976256512	27808	66.0613	21.7361	23.3598	117.3728	-45.7965	37.30
3313947699887831808	27848	66.0932	17.0788	19.8786	99.9086	-26.6532	39.83
3313662892016181504	27859	66.1185	16.8861	22.1282	113.0887	-25.0414	37.70
3312783557591565440	27991	66.4060	15.9409	20.8702	106.8848	-25.0698	39.60
145293177350363264	28033	66.5775	21.4703	21.4611	103.5366	-37.8687	38.21
3313689417734366720	28099	66.6676	16.7468	21.9436	108.8452	-28.0853	38.69
3312709374919349248	28205	66.9000	15.5891	21.1292	105.2035	-23.8015	39.10
3306922954457367936	28237	66.9424	11.7364	21.6354	110.0126	-12.4712	39.663
3314109912215994112	28344	67.2017	17.2853	21.6371	108.6998	-28.4150	39.171
3314212063714381056	28406	67.3769	17.8630	21.4936	106.0916	-31.9674	37.50
3305871821341047808	28608	67.7387	10.7517	21.2031	102.9851	-10.8185	39.00
3307815001984777088	28635	67.8727	13.9034	18.5638	89.9478	-17.3586	39.245
3307528029449757056	28911	68.4448	13.2518	21.6651	102.8164	-17.4181	35.00
3312575681175439616	28992	68.6476	15.5045	21.7450	101.1236	-26.7425	40.314
146677874804442240	29419	69.7142	23.1497	22.9950	105.4934	-54.1927	39.08
3405113740864365440	30589	72.3842	15.8886	20.8788	86.7435	-25.5009	42.717
3404812680839290368	30712	72.6413	15.0833	21.1649	88.9776	-23.3618	42.59
3405220084257276416	30738	72.7026	16.2103	20.0725	83.0972	-26.2501	44.20
3404850785786832512	30809	72.8470	15.4334	16.4489	65.8227	-18.1965	43.432
3408463506117452544	31236	73.7435	19.4853	15.9153	62.8383	-28.9176	35.00

Appendix B

Units

In the name of practicality, SI-units are not used in this project, due to the greatness of most values within astronomy if expressed in these units. Instead, the following units are being used (all values are taken from Lennart Lindegren's "Dynamical Astronomy, Lecture Notes for ASTM13, ", 2014);

Mass

The masses of bodies and potentials are expressed in solar masses, $M_\odot$, with one solar mass being equal to $1M_\odot = 1.989 \cdot 10^{30}$ kg.

Distance

Distances are measured in parsec, pc, with one parsec being equal to 1 pc = $3.0856776 \cdot 10^{13}$ km.

Velocity and Acceleration

Due to the velocity range of the stars in the Milky Way, the unit suitable is km/s. The acceleration unit then naturally becomes km/s^2.

Time

Since the units for distance and velocity are now given, we can calculate the natural unit to use for time by dividing the distance with the velocity, i.e.

$$t = \frac{1 \text{ pc}}{\text{km/s}} = 3.0856776 \cdot 10^{13} \text{ s} = 9.7779223 \cdot 10^{5} \text{ yr}. \tag{B.1}$$

Noticeably, this is very close to 1 Myr (10^6 years), but in order to maintain accuracy the time is divided by a factor of 0.9778, and the unit thus becomes Myr.

The Gravitational Constant

Given all the units above, the gravitational constant G can be calculated to

$$G = 0.00430091722 \text{ pc } (\text{km/s})^2 \ M_{\cdot}^{-1}. \tag{B.2}$$

Coordinate System

For simplicities sake, all simulation were run in the Galactocentric frame, with the Milky Way centre at origo and the Sun defining the direction of the x-axis. The unit vector used was 1 parsec for all axes.

Appendix C

Additional Plots

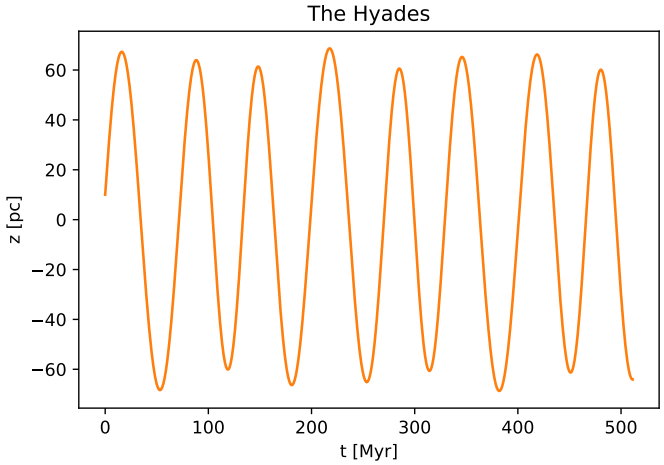

(a) Height z (relative to the galactic plane) as a function of time t. The height is expressed in parsec and the time in Myr. This is a more detailed version of the height in figure 4.1a (green line).

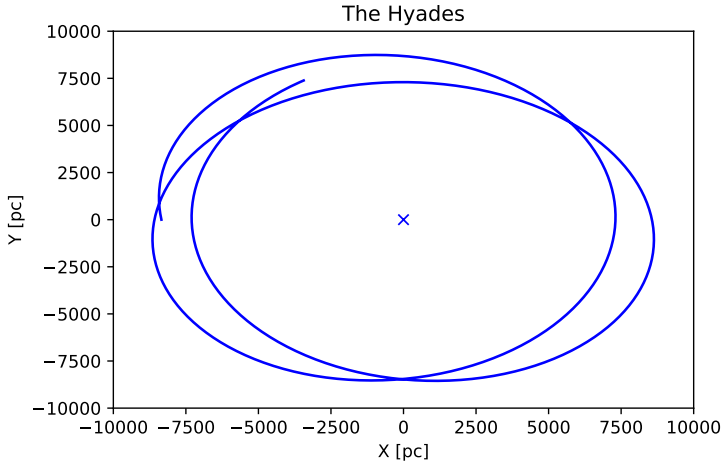

(b) Top-down view of the orbit of the Hyades open cluster over a 500 Myr timespan, with x-coordinate on the horizontal axis and y-coordinate on the vertical axis, both expressed in parsec.

Figure C.1: (a) Height against time- and (b) x-y plot of the Hyades open cluster in the Milky Way, over a timespan of 500 Myr. The plots are made in a galactocentric coordinate system.

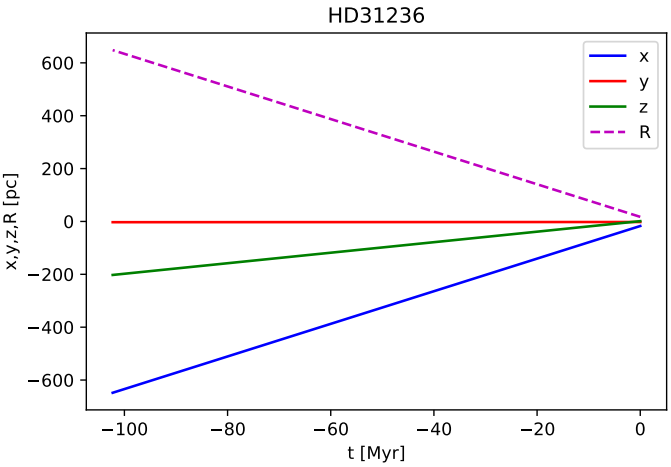

(a) x-, y-, and z-values (in blue, red and green respectively), as well as radius $R = \sqrt{x^2 + y^2}$ (dashed magenta line), as a function of time t. The orbits are integrated backwards in time in order to give an indication of the origin of the star. All four lines appear linear, which indicates that the star has not interacted very much at all with other bodies or potentials in the simulation. In comparison to integrating in positive time-direction (figure 4.4), y is still roughly constant at time $y \sim 0$, but since x is now negative and $R \geq 0$, the two values do not coincide for all negative times.

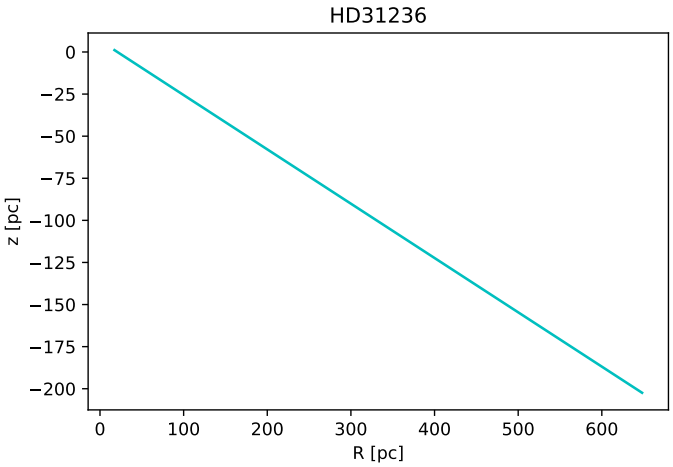

(b) Radius-to-height plot of HD31236, where $R = x^2 + y^2$ is the radius and z is the height. Both axis are in parsec. The linearity of the plot suggests that the star has not interacted very much at all with potentials or other stars in the N-body. This in turn points to the star not being a true member of the Hyades, but merely passing through.

Figure C.2: x, y, z, R) against time t, as well as height z against two-dimensional radius R, of the star HD31236, integrated 100 Myr backwards in time.

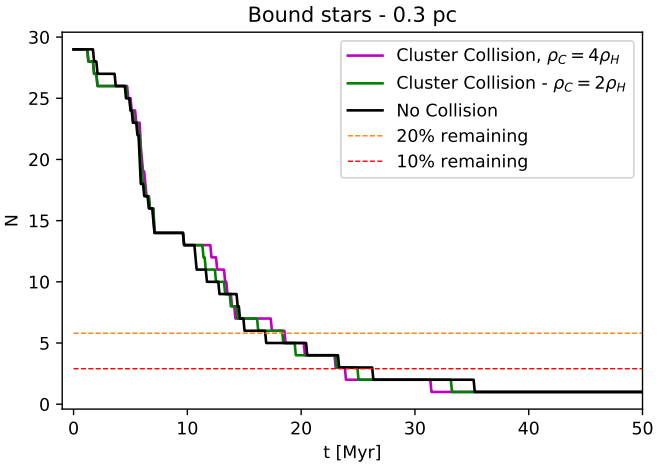

(a) Number of bound stars in The Hyades, when colliding with a cluster with a centre-to-centre distance of $r \sim 0.3$ pc at the time of impact, as a function of time.

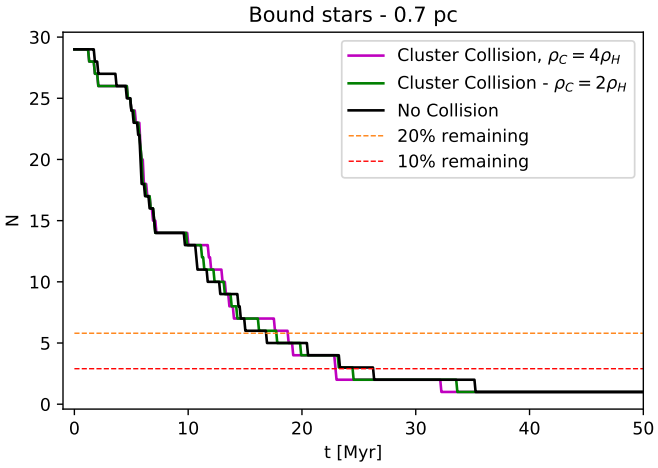

(b) Number of bound stars in The Hyades as a function of time, when colliding with a cluster. Here, the centre-to-centre distance is $r \sim 0.7$ pc at the time of impact.

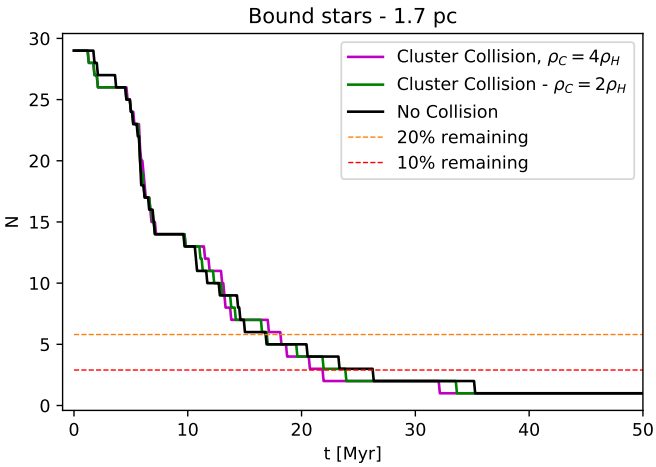

(c) Number of bound stars in The Hyades as a function of time, with a impact centre-to-centre distance of ~ 1.7 pc.

Figure C.3: Number of bound stars N (stars within the tidal radius r_t) in the Hyades open cluster (vertical axis) as a function of time t in Myr (horizontal axis). No cluster collision in black, collision with a cluster of the same density and volume in green ($\rho_C = 2\rho_H$, $800M\odot$), and collision with a cluster with a density of $\rho_C = 4\rho_H$ ($1600M\odot$). The time of the collision is 0.9 Myr into the simulation, and the relative velocity of the clusters is $v \sim 15$ km/s. Threshold values for 20% and 10% of the initial number of bound stars marked as dashed orange and dashed red line respectively. The plots are cropped at $t = 50$ Myr, since all N remain constant after this point.